Human PATHOLOGY

www.elsevier.com/locate/humpath

ELSEVIER

Original contribution

Neuroendocrine carcinoma and mixed neuroendocrine–non-neuroendocrine neoplasm of the stomach: a clinicopathological and exome sequencing study☆

Sonoko Ishida MD [a,b], Masayuki Akita MD, PhD [a,c], Kohei Fujikura MD, PhD [a], Masato Komatsu MD, PhD [a], Ryuichiro Sawada MD, PhD [a,b], Hisayuki Matsumoto BSc [d], Jun Saegusa MD, PhD [d], Tomoo Itoh MD, PhD [a], Yoshihiro Kakeji MD, PhD [b], Yoh Zen MD, PhD, FRCPath [a,e,*]

[a] *Department of Diagnostic Pathology, Kobe University Graduate School of Medicine, Kobe 650-0017, Japan*
[b] *Department of Gastroenterological Surgery, Kobe University Graduate School of Medicine, Kobe 650-0017, Japan*
[c] *Department of Hepato-Biliary-Pancreatic Surgery, Kobe University Graduate School of Medicine, Kobe 650-0017, Japan*
[d] *Department of Laboratory Medicine, Kobe University Graduate School of Medicine, Kobe 650-0017, Japan*
[e] *Institute of Liver Studies, King's College Hospital & King's College London, London SE5 9RS, UK*

Received 12 October 2020; revised 9 December 2020; accepted 18 December 2020

Available online 21 January 2021

Keywords:
TP53;
Neuroendocrine;
Adenoendocrine carcinoma;
MEN1;
Gastric cancer

Summary The gene mutation profiles of gastric neuroendocrine neoplasms are incompletely understood. The purpose of this study was to characterize the molecular pathology of poorly differentiated neuroendocrine carcinoma (NEC) and mixed neuroendocrine–non-neuroendocrine neoplasm (MiNEN) of the stomach. Surgical cases of gastric NEC (n = 7) and MiNEN (n = 6) were examined by clinical review, immunohistochemistry, microsatellite instability (MSI) analysis and whole-exome sequencing. NEC cases consisted of small- (n = 2) and large-cell types (n = 4). All cases of MiNEN were histologically composed of large-cell type NEC and tubular adenocarcinoma. Whole-exome sequencing analysis detected recurrent mutations in *TP53* in 8 cases (62%), and they were more frequently observed in MiNEN than in NEC (100% vs. 29%). Frameshift mutations of *APC* were observed in two cases of MiNEN. One case of large-cell type NEC had a frameshift mutation with loss of heterozygosity in *RB1*. The other mutated genes (e.g., *ARID1* and *KRAS*) were detected in a

☆ Disclosures: None.

* Corresponding author. Institute of Liver Studies King's College Hospital, London, UK
E-mail address: yoh.1.zen@kcl.ac.uk (Y. Zen).

https://doi.org/10.1016/j.humpath.2020.12.008

single case each. A high level of MSI was confirmed in one case of MiNEN, which harbored mutations in two well-differentiated neuroendocrine tumor (NET)-related genes (*MEN1* and *ATRX1*). In cases of MiNEN, two histological components shared mutations in *TP53*, *APC* and *ZNF521*, whereas alterations in *CTNNB1*, *KMT2C*, *PTEN* and *SPEN* were observed in neuroendocrine components only. In conclusion, *TP53* is a single, frequently mutated gene in gastric NEC and MiNEN, and alterations in other genes are less common, resembling the mutation profiles of gastric adenocarcinomas. Gene mutations frequently observed in well-differentiated NET were uncommon but not entirely exclusive.

1. Introduction

Neuroendocrine neoplasms have two major diagnostic categories. Neuroendocrine tumor (NET) is a well-differentiated group with an indolent clinical course and relatively monomorphic histological appearance [1–3]. Neuroendocrine carcinoma (NEC) is a poorly differentiated, aggressive malignancy with immunohistochemical evidence of neuroendocrine differentiation, and is further classified into small- and large-cell types, histologically corresponding to small-cell carcinoma and large-cell neuroendocrine carcinoma of the lungs, respectively [1–3]. Another less common category is mixed neuroendocrine–non-neuroendocrine neoplasm (MiNEN), in which a neuroendocrine neoplasm is combined with a non-neuroendocrine component, each element constituting ≥30% of the entire tumor. Cases traditionally diagnosed as mixed adeno-neuroendocrine carcinoma are currently included in that group.

Neuroendocrine neoplasms are increasingly diagnosed worldwide. In the gastrointestinal tract, NEC and MiNEN more frequently develop in the colorectum than in other areas, including the stomach and small intestine. In contrast, the lungs, pancreas, and small intestine are the three prevalent anatomical locations for well-differentiated NET [4–6]. Of note, the incidence of NET in some organs differs among races, with rectal NET more commonly found in Asia than in Europe and USA, whereas small-intestinal NET more frequently develops in Caucasians than in Asians [5,6].

It is controversial whether NET and NEC belong to a single tumor entity or are two distinct neoplasms. Another question is whether there are molecular differences in neuroendocrine neoplasms among organs despite the similar microscopic appearance. Recent deep sequencing studies provided insights into these two aspects. The lack of mutations in NET-related genes (e.g., *MEN1*, *ATRX* and *DAXX*) in NEC of the lungs and pancreas suggested that NEC and NET are biologically distinct [7–10]. In addition, the incidence of *MEN1* alterations in NET differs among organs, and mutations in *ATRX* and *DAXX* are almost restricted to pancreatic NET [9,11,12], suggesting that different molecular events drive the development of NET in individual organs.

However, molecular data of neuroendocrine neoplasms are mainly based on investigations of pulmonary and pancreatic lesions, whereas the genetic features of neuroendocrine neoplasms in other organs are incompletely understood. In the present study, the molecular pathology of NEC and MiNEN of the stomach was investigated using whole-exome sequencing.

2. Materials and methods

2.1. Case selection

This study was approved by the ethics committee of Kobe University Graduate School of Medicine. The study cohort consisted of 13 consecutive patients with gastric NEC (n = 7) or MiNEN (n = 6) who underwent gastrectomy at Kobe University Hospital between 2000 and 2017. Cases were identified by searching pathology archives and only surgical cases were selected considering the large amount of DNA required for deep sequencing.

2.2. Evaluation of clinicopathologic features

Clinical data, treatment history, and outcomes were retrieved from electronic medical records. The pathology reports and histology slides of all patients were also reviewed in terms of tumor size, location, degree of microscopic lymphovascular invasion (0, none: 1, mild; 2, moderate; 3, severe), and lymph node metastasis. Original stained slides of chromogranin A (stained by clone DAK-A3; Dako Cytomation, Glostrup, Denmark), synaptophysin (clone MRQ-40; Roche Diagnostics, Basel, Switzerland), and CD56 (clone MRQ-42; Roche Diagnostics) were reviewed and evaluated as positive (expressed in ≥5% of tumor cells) or negative (<5% of tumor cells). Ki67-stained slides (stained by clone MIB1; Dako Cytomation) were also reviewed. The Ki67 labeling index (5% intervals) at a hot spot with >500 tumor cells and mitotic counts per 10 high-power fields were calculated in neuroendocrine components.

2.3. Immunostaining

Additional immunostaining for p53 and HER2 was performed on the most representative section from each case using Benchmark XT (Ventana Medical Systems, Tucson, AZ, USA) or Bond Max (Leica Microsystems, Wetzlar, Germany). The used antibodies were as follows: p53 (clone DO-7; Leica Microsystems) and HER2 (clone 4B5; Roche Diagnostics). The expression of p53 was classified into "normal", with occasional weakly stained cells, "positive", with diffuse nuclear staining, and "loss", with entirely negative staining suggesting null-type mutations, and the latter two were considered to be abnormal p53 expression. The HER2 overexpression status was scored as 0 (negative), 1 + (negative), 2 + (equivocal), or 3 + (positive) according to a previously reported method [13]. In cases of MiNEN, expression of p53 and HER2 was separately evaluated in neuroendocrine and non-neuroendocrine components. Additional immunostaining for mismatch repair (MMR) proteins was performed in cases that had high microsatellite instability (MSI) by molecular assays. The used antibodies were as follows: MLH1 (clone G168-728; Cell Marque, Rocklin, CA), MSH2 (clone G219-1129; Cell Marque), MSH6 (clone EP49; Dako Cytomation), and PMS2 (clone EP51; Dako Cytomation).

2.4. Exome sequencing

Genomic DNA extracted from tumor tissue in individual cases was applied to a whole-exome sequencing protocol according to the previously described method [14–16]. In cases of MiNEN with two distinctly recognized components, each element was separately analyzed. In cases of MiNEN in which two components were intermixed, areas composed purely of a neuroendocrine component were selected for DNA extraction. Ten 10-μm-thick sections were obtained from formalin-fixed paraffin-embedded tissue blocks, and areas composed of a large proportion of tumor cells (>50%) were selected under a microscope. DNA extraction was performed using the GeneRead DNA FFPE kit (Qiagen, Hilden, Germany) following the manufacturer's protocol. DNA content was measured using the Qubit® 2.0 fluorometer (Thermo Fisher Scientific, Waltham, MA, USA). The Agilent SureSelect Exon V6 target enrichment system was used to enrich a 60-Mb exome following Illumina Hiseq X platform sequencing using 150-bp paired-end reads. At least 12 Gb of raw read data were produced for all samples. BWA (http://bio-bwa.sourceforge.net/) and SAMtools (http://samtools.sourceforge.net/) were used for read alignment and single nucleotide variation (SNV) calling, respectively, using fully validated filtering criteria for identifying high-quality DNA variants. The variants were filtered for synonymous, non-synonymous, stop-causing or stop-loss variants in exonic or essential splice site locations with a variant allele frequency of at least 5%. An allele frequency cutoff of 5% was selected to minimize the inclusion of sequencing artifacts related to formalin fixation. SNVs and indels of well-known pathogenic genes were selected from the whole-exome sequencing results. Coverage of these variants ≥20x was filtered by COSMIC, the Japanese 3500 Genome project and Tohoku Medical Megabiobank Organization databases, to exclude single nucleotide polymorphisms.

2.5. MSI analysis

Tumor DNA extracted from formalin-fixed paraffin-embedded specimens was also applied to PCR/capillary electrophoresis-based MSI analysis using a pentaplex panel of microsatellite markers (BAT25, BAT26, NR21, NR24 and NR27). High MSI was scored if at least two of the five markers exhibited genetic instability.

2.6. Statistical analysis

A chi-square test was applied to compare the frequency of *TP53* mutations between NEC and MiNEN groups.

3. Results

3.1. Clinical features

The clinical features of gastric NEC (cases 1–7) and MiNEN (cases 8–13) are summarized in Table 1. All patients were adults with a median age of 70 years (range 57–93). Four patients (cases 3, 11–13) had a history of malignancy in other organs, but none exhibited neuroendocrine differentiation. Synchronous malignancy was also confirmed in three cases and they were resected at the same time of gastrectomy for NEC/MiNEN. Diagnostic gastric biopsy samples were interpreted as NEC (n = 3; cases 5, 6, and 12), adenocarcinoma (n = 9; cases 1, 3, 4, 7–11, and 13) and poorly differentiated carcinoma with features suggestive of squamous differentiation (n = 1; case 2). Underlying chronic atrophic gastritis was suspected in 9 cases by endoscopic findings, and it was confirmed histologically by pre-operative biopsy and/or resected specimen. Four patients (cases 8, 10, 12 and 13) were positive for *Helicobac er p lori* infection, but it was not tested in the remaining patients. All patients underwent surgical resection, and two also received neoadjuvant chemotherapy with cisplatin and etoposide prior to surgery. In those cases, postchemotherapy specimens were used for the following studies.

3.2. Pathological characteristics

As summarized in Table 2, NEC cases consisted of small- (n = 2) and large-cell types (n = 4) (Fig. 1A). Cases 1 and 5 also had small foci of adenocarcinoma (<10% of the neoplasm), which did not meet the criteria of

Table 1 Clinical features and outcomes.

Pt	Age/gender	Diagnosis	Other malignancies	Chronic atrophic gastritis	Neoadjuvant chemotherapy	Adjuvant chemotherapy	Follow-up (month)	Outcome
1	68F	NEC	None	No	None	None	2.6	DOD
2	64M	NEC	None	No	None	None	7.4	DOD
3	63M	NEC	Lung adenocarcinoma (past); esophageal SCC (synchronous)	Yes	None	None	10.0	DOA
4	70M	NEC	Gastric adenocarcinoma (synchronous)	Yes	None	None	39.7	DOA
5	66M	NEC	None	No	None	None	4.9	DOD
6	58M	NEC	None	Yes	CDDP + VP16	S-1	86.0	DOD
7	75M	NEC	None	No	None	CPT-11+CDDP; S-1; PTX	24.6	DOO
8	81M	MiNEN	None	Yes	CDDP + VP16	None	34.6	Alive
9	93F	MiNEN	None	Yes	None	None	2.3	Alive
10	85M	MiNEN	None	Yes	None	None	56.6	Alive
11	71M	MiNEN	Hypopharyngeal SCC (past); gastric adenocarcinoma (synchronous)	Yes	None	CPT-11+CDDP	55.8	Alive
12	80M	MiNEN	Hepatocellular carcinoma (past)	Yes	None	None	8.1	DOA
13	69M	MiNEN	Esophageal SCC (past)	Yes	None	None	8.9	DOA

SCC, squamous cell carcinoma; CDDP, cisplatin; VP16, etoposide; CPT-11, Irinotecan; PTX, Paclitaxel; DOD, died of the disease (gastric NEC/MiNEN); DOA, died of another diseases; NEC, neuroendocrine carcinoma; MiNEN, mixed neuroendocrine–non-neuroendocrine neoplasm.

MiNEN (each component should be $\geq$ 30%). Case 7 demonstrated abnormal spindle-cell transformation of neuroendocrine cancer cells, and that area was immunoreactive to pan-cytokeratins (Cam5.2 and AE1/AE3) and synaptophysin (Fig. 1B). Neuroendocrine components in all cases of MiNEN were large-cell type, and their proportions ranged from 30% to 50%. No components of well-differentiated NET were identified. Non-neuroendocrine components were all conventional tubular adenocarcinoma and one case also had foci of poorly differentiated adenocarcinoma. All but one case of mixed cancer (including cases 1 and 5) exhibited a collision pattern, in which a NEC component was next to an adenocarcinoma element (Fig. 2A and B). In case 9 with a combined pattern, two components intermixed (Fig. 2C). However, there were several foci consisting purely of neuroendocrine components and those areas were used for the sequencing studies described in the following context.

Tumors varied in location and size (median size 30 mm; range: 15−155 mm) (Table 2). Neuroendocrine differentiation was confirmed by the immunohistochemical expression of chromogranin A (n = 2), synaptophysin (n = 5) or both (n = 6). CD56 was also expressed in 9 cases. Microscopic lymphovascular invasion was common. Regarding the tumor stage, the depth of invasion was down to the submucosal layer in 3 cases (pT1b; 23%), the muscularis propria in 3 cases (pT2; 23%), and the subserosal layer in 7 cases (pT3; 54%). No case had serosal surface involvement. Lymph node metastasis was confirmed in 9 cases (69%). Cases 1, 7, and 11 were classified as M1 because of liver metastasis or para-aortic nodal involvement. In two cases with neoadjuvant chemotherapy, tumor necrosis and degeneration were only focally observed.

3.3. Immunohistochemistry for p53 and HER2

As shown in Fig. 3, abnormal expression of p53 was observed in 9 cases (69%), and p53 immunoreactivity was similar in adenocarcinoma and neuroendocrine components in all cases of MiNEN. In case 11, HER2 was strongly expressed in adenocarcinoma (score 3) but not in the neuroendocrine component (score 0). The other cases were considered to be HER2-negative (scores 0 or 1).

3.4. Outcome

As shown in Table 1, 6 patients died of gastric NEC/MiNEN in the median period of 8.7 months after surgery (range: 2.6−86.0 months). Three patients died of another condition (case 4, lung cancer; case 12, intestinal

Table 2 Pathological features.

Pt	Neuroendocrine component (type, %)	Adenocarcinoma component (type, distribution)	Location	Size (mm)	Lymphatic invasion*	Venous invasion*	Ki67 index (%)	Mitotic counts (/10 hpf)	pT	pN	cM	Stage	R
1	Small cell type (>90%)	Tubular, moderately diff.; collision	Middle, lesser curvature	140	3	3	50	33	3	1	1 (liver)	IV	R1
2	Large cell type (100%)	None	Upper, anterior wall	155	3	3	25	9	3	3a	0	IIIB	R0
3	Large cell type (100%)	None	Upper, posterior wall	30	1	3	40	4	2	1	0	IIA	R0
4	Large cell type (100%)	None	Lower, greater curvature	18	0	1	50	16	1b	0	0	IA	R0
5	Large cell type (>90%)	Tubular, well diff.; collision	Lower, lesser curvature	37	2	2	25	28	2	2	0	IIB	R0
6	Small cell type (100%)	None	Lower, greater curvature	35	0	0	60	21	2	2	0	IIB	R0
7	Large cell type with spindle cells (100%)	None	Lower, circumferential	90	1	3	40	19	3	0	1 (para-aorta LN)	IV	R2
8	Large cell type (30%)	Tubular well diff.; collision	Middle, posterior wall	35	0	2	95	24	3	1	0	IIB	R0
9	Large cell type (50%)	Mixed tubular and poorly cohesive; combined	Middle, anterior wall	90	2	2	50	16	3	3a	0	IIIB	R0
10	Large cell type (30%)	Tubular, moderately diff.; collision	Upper, lesser curvature	31	0	1	40	2	3	0	0	IIA	R0
11	Large cell type (30%)	Tubular, moderately diff.; collision	Lower, greater curvature	15	2	2	80	11	3	2	1 (liver)	IV	R2
12	Large cell type (30%)	Tubular, moderately diff.; collision	Middle, anterior wall	30	1	0	90	22	1b	1	0	IB	R0
13	Large cell type (40%)	Tubular, well diff.; collision	Upper, lesser curvature	30	0	0	70	5	1b	0	0	IA	R0

*, semiquantitative analysis (0, none; 1, mild; 2, moderate; 3, severe); LN, lymph node.

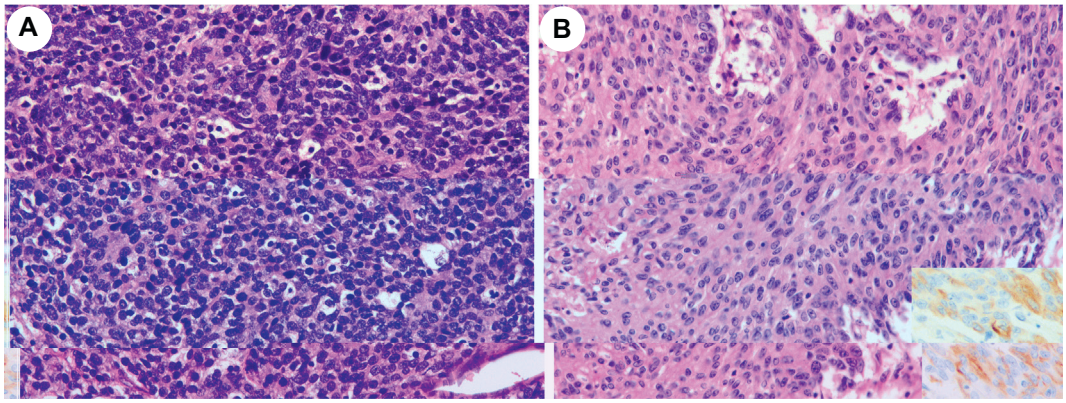

Fig. 1 Histopathology of NEC of the stomach. (A) In a case of small-cell type NEC, round-shaped cancer cells with dark nuclei, coarse chromatin and indistinct nucleoli are arranged in a diffuse fashion. No glandular differentiation is observed (case 1; H&E; original magnification ×200). (B) A case of large-cell type NEC is associated with spindle cell transformation, which is immunoreactive to synaptophysin (inset) (case 7; H&E and synaptophysin immunostaining; original magnification ×200).

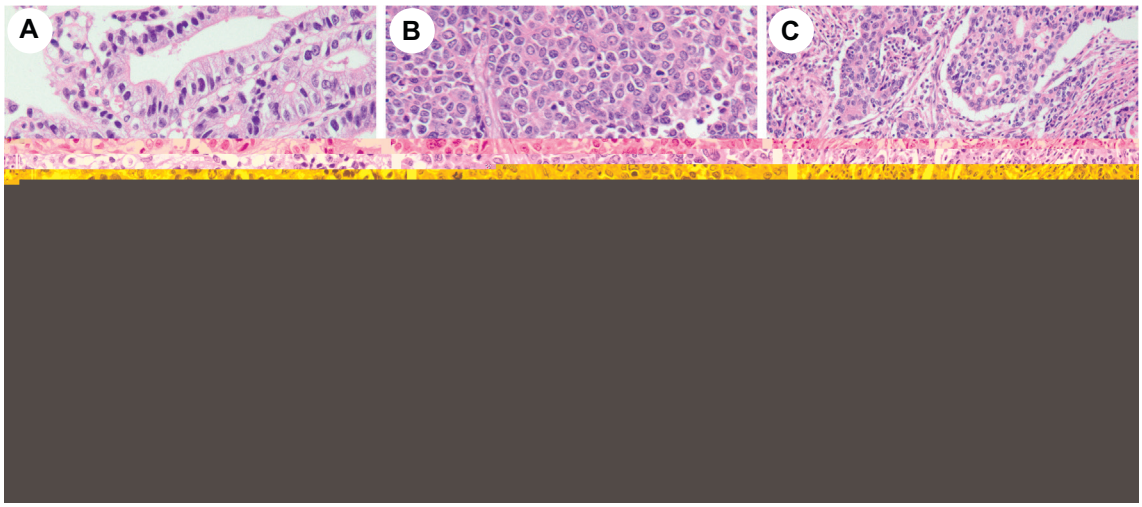

Fig. 2 Histopathology of MiNEN. (A and B) A tumor of collision-type MiNEN consists of well-differentiated adenocarcinoma (A) and large-cell type NEC (B). This is an MSI-high tumor (case 8; H&E; original magnification ×200). (C) In a tumor of combined-type MiNEN, adenocarcinoma and neuroendocrine components are intermixed. Tubule formation confirming glandular differentiation and solid nests representing a neuroendocrine element are observed (case 9, H&E, original magnification ×100). MiNEN, mixed neuroendocrine–non-neuroendocrine neoplasm.

obstruction; case 13, unknown cause). The remaining four patients with MiNEN were alive at the median period of 45.2 months (range: 2.3−56.6).

3.5. MSI

A single case of MiNEN (case 8) was judged to be MSI-high cancer with an instable pattern of electrophoresis confirmed by four of the five markers tested. Immunostaining confirmed the loss of MSH2 and MSH6 expression, whereas the expression of MLH1 and PMS2 remained (Fig. 4). No genetic instability was observed in any other cases.

3.6. Whole-exome sequencing

Deep sequencing studies of neuroendocrine components were successful in all cases. After manual inspection by the Integrative Genomics Viewer to exclude false-positive findings, the whole-exome sequencing analysis detected recurrent mutations in *TP53* (n = 8; 62%): 6 missense, 1 nonsense, and 1 frameshift mutation (Fig. 3 and Table 3). *TP53* mutations were more commonly found in MiNEN (6/6 cases; 100%) than in NEC (2/7 cases; 29%; $P = 0.039$). A good correlation between *TP53* mutations and p53 immunohistochemistry was observed except in case 1, in which p53 was diffusely positive on immunostaining, but no exonic mutations were confirmed by sequencing

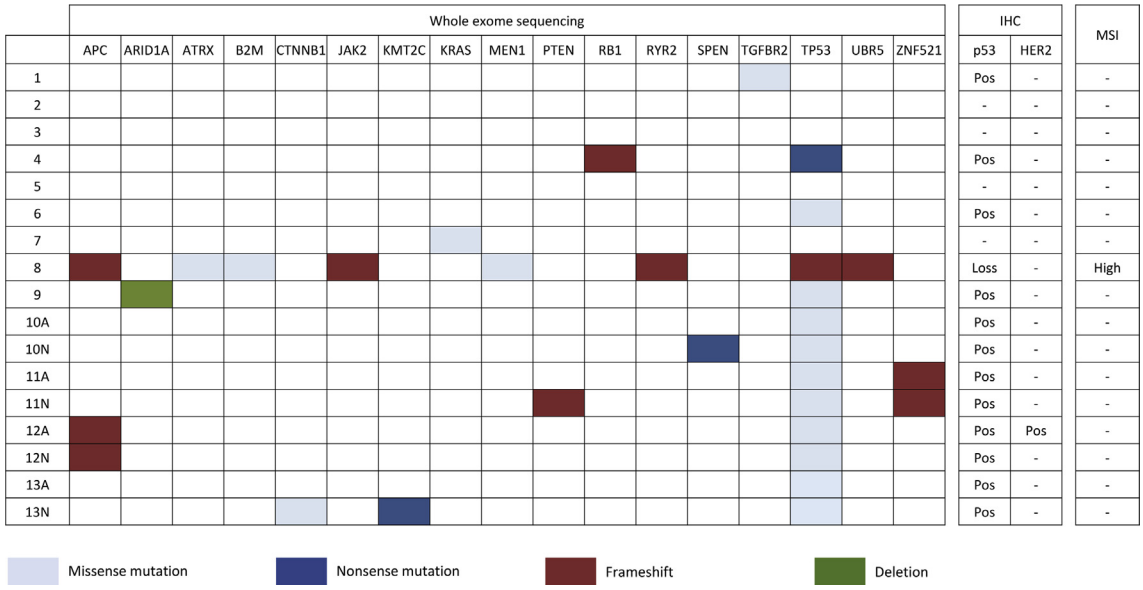

Fig. 3 Results of exome sequencing, immunohistochemistry, and MSI analysis. In immunohistochemical analysis, the diffuse expression (pos) and complete loss of expression (loss) are considered abnormal p53 expression.

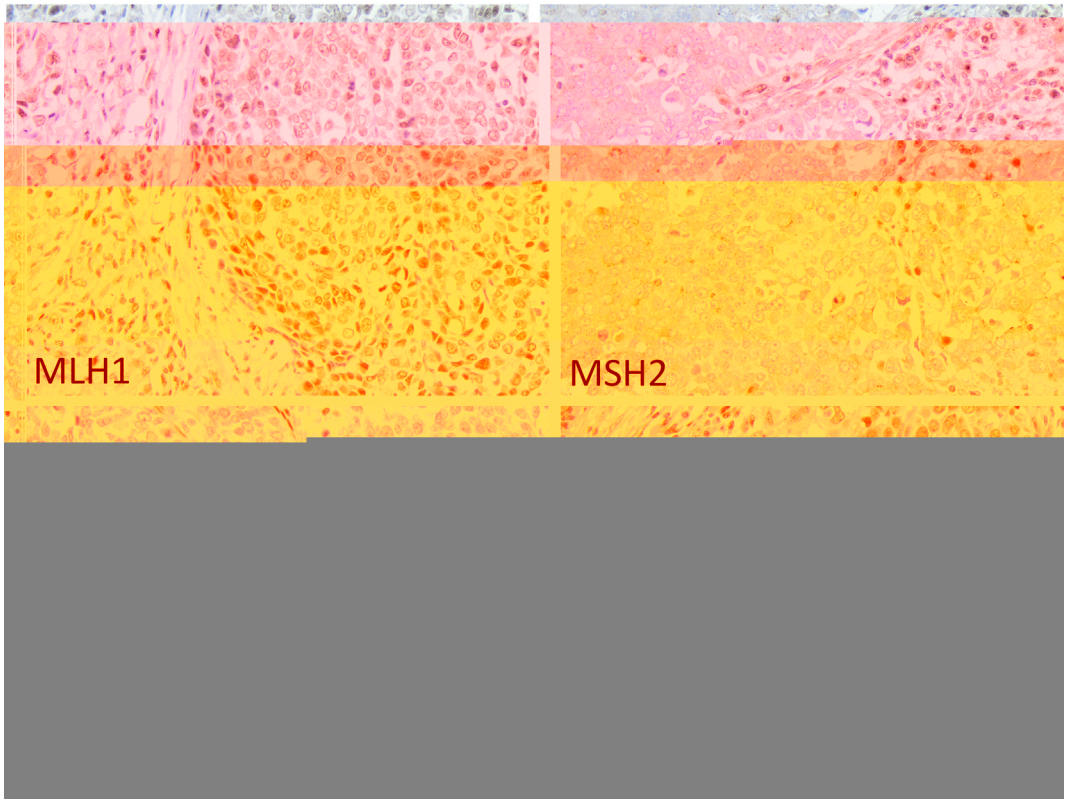

Fig. 4 MMR protein expression in case 8. Expression of MLH1 and PMS2 remained, whereas that of MSH2 and MSH6 was lost. Infiltrating lymphocytes or stromal cells in the background are immunoreactive to MSH2 and MSH6 (internal controls) (original magnification ×200). MMR, mismatch repair.

(Fig. 3). Frameshift mutations in *APC* were observed in two cases. MSI-high MiNEN (case 8) had 8 mutations, two of which were present in NET-related genes, *MEN1* and *ATRX1,* the former associated with a loss of heterozygosity. A frameshift mutation in *RB1* with loss of heterozygosity was also confirmed in case 4. Other gene alterations were observed in a single case each. The detected gene mutations are summarized in Table 3.

Table 3 Gene mutations detected.

Gene	Case	Mutation
APC	8	NM_001127511: exon 14: c.3131delA: p.Q1044fs
APC	12	NM_001127511: exon 14: c.4719dupA: p.A1573fs
ARID1A	9	NM_006015: exon 20: c.6796delT: p.L2266X
ATRX	8	NM_000489: exon 28: c.C6253T: p.R2085C
B2M	8	NM_004048: exon 2: c.T133C: p.C45R
CTNNB1	13	NM_001904: exon 3: c.C98G: p.S33C
JAK2	8	NM_004972: exon 13: c.1736delT: p.L579fs
KMT2C	13	NM_170606: exon 23: c.C3709T: p.R1237X
KRAS	7	NM_033360: exon 2: c.G34T: p.G12C
MEN1	8	NM_000244: exon 2: c.T394C: p.S132P
PTEN	11	NM_000314: exon 8: c.963dupA, p.T321fs
RB1	4	NM_000321: exon 19: c.1960_1960del: p.V654fs
RYR2	8	NM_001035: exon 104: c.14758dupT: p.L4919fs
SPEN	10	NM_015001: exon 11: c.C9541T: p.Q3181X
TGFBR2	1	NM_001024847: exon 7: c.G1565A: p.R522Q
TP53	4	NM_001126112: exon 9: c.T981G: p.Y327X
TP53	6	NM_001126112: exon 5: c.G524A: p.R175H
TP53	8	NM_001126112: exon 8: c.790_791del: p.L264fs
TP53	9	NM_001126112: exon 5: c.G524A: p.R175H
TP53	10	NM_001126112: exon 5: c.T434C: p.L145P
TP53	11	NM_001126112: exon 5: c.C452A: p.P151H
TP53	12	NM_001126112: exon 7: c.C742T: p.R248W
TP53	13	NM_001126112: exon4: c.C215G: p.P72R
UBR5	8	NM_015902: exon 45: c.6360delA: p.K2120fs
ZNF521	11	NM_015461: exon 4: c.546delG: p.A182fs

Adenocarcinoma components of collision type MiNEN were separately analyzed. Case 9 with an intermixed, combined type morphology was excluded. Sequencing of the adenocarcinoma component of cases 8 was unsuccessful because of the low quality or quantity of DNA. Thus, paired samples were compared in cases 10−13. *TP53* was mutated in all of those cases, and the same mutation was detected in both neuroendocrine and adenocarcinoma components. Mutations in *APC* and *ZNF521* were also identified in the two components. In contrast, alterations of *CTNNB1*, *KMT2C*, *PTEN* and *SPEN* were observed in neuroendocrine components only. Mutations that were present in an adenocarcinoma component only were not observed.

4. Discussion

The present study identified *TP53* as a single cancer-related gene frequently mutated in gastric NEC and MiNEN. *TP53* mutations are also common in NEC/MiNEN in other organs, and the mutation rate of gastric NEC/MiNEN (62%) is lower than that of pulmonary small-cell carcinoma (>95%) [8] and pulmonary large-cell neuroendocrine carcinoma (∼80%) [7], and comparable to that of pancreatic NEC/MiNEN (∼60%) [9,10] and colorectal NEC/MiNEN (∼50%) [17]. Of note, *TP53* was more frequently mutated in MiNEN than in NEC in the present study. However, a previous exome sequencing study of 6 cases of gastric NEC found *TP53* mutations in all cases examined [18]. In addition, case 1 in the present study demonstrated diffuse immunoreactivity to p53 despite the lack of *TP53* mutation, suggesting inhibition of p53 by non-exonic genetic alteration.

RB1 is another gene frequently mutated in pulmonary small-cell carcinoma (>95%) [8,19], pulmonary large-cell neuroendocrine carcinoma (∼40%) [9,19] and pancreatic NEC (∼40%) [9,10]. In the present study, a single case had *RB1* mutation along with loss of heterozygosity. In a previous study, *RB1* mutation was identified in 1 of 25 cases of colorectal NEC/MiNEN, but it was a heterologous deletion and therefore less likely to be pathognomonic [17]. Based on the frequencies of mutations in *TP53* and *RB1*, gastric NEC/MiNEN are more similar to their colorectal counterparts than to pulmonary or pancreatic NEC/MiNEN. Unlike our cases, colorectal NEC/MiNEN also had recurrent mutations in *BRAF* (37%), *KRAS* (21%), and *APC* (16%) [17]. That difference may represent distinct molecular features among conventional carcinomas of the two organs. *BRAF*, *KRAS,* and *APC* are common driver genes of colorectal cancers [20], whereas mutations in non-*TP53* genes are less common (<10%) in gastric adenocarcinoma [21,22].

There is growing evidence that NEC is distinct from NET. This is most notable in pancreatic neoplasms. Pancreatic NET has mutations in *MEN1* (43%), *DAXX* (28%), *ATRX* (11%), *TSC2* (6%), and *PTEN* (5%) [11,23], whereas pancreatic NEC typically lacks such abnormalities, and instead has mutations in *TP53* and *RB1* [9]. Likewise, pulmonary NET has mutations in *MEN1* in 18% of cases, but usually lacks alterations of *TP53* and *RB1* [11]. However, a similar comparison is difficult for

gastrointestinal neuroendocrine neoplasms because only a handful of genes are recurrently mutated in gastrointestinal NET: *BCOR* (6%) and *CDKN1B* (4%) in small intestinal NET; *ATM* (15%) in colorectal NET [11].

To our knowledge, four previous studies examined the gene mutation profiles of gastric NET using a next-generation sequencing protocol [11,24–26], and two provided detailed results [24,25]. Combining the two studies, 22 cases were examined in total, and sporadic mutations were found in *TP53* (3/22 cases; 14%), *RB1* (2/22; 9%), and *SMAD4* (2/22; 9%). Mutations in NET-related genes were also rare: *MEN1* (1/15; 7%), *ATRX* (1/15; 7%), *TSC2* (1/15; 7%), and *PETN* (1/22; 5%) (the former three genes were not examined in one study [25]). Half of the cases (11/22; 50%) did not harbor mutations in any of the genes tested. Although the molecular features of gastric NET remain to be determined, considering the other data, NEC and MiNEN share molecular features with conventional cancers of individual organs, supporting the idea that NEC is more closely related to conventional carcinomas than to NET.

One case of MSI-high MiNEN had mutations in *MEN1* and *ATRX*. These genes require homozygous mutations for tumorigenesis. As the identified mutation in *MEN1* was associated with a loss of heterozygosity and *ATRX* is located on the X chromosome (the patient was male and had one X chromosome), these genes were likely significantly suppressed. Sporadic cases of NEC/MiNEN with a NET-related gene mutation have also been reported in other organs [27,28]. These cases suggest that mutations in NET-related genes in conventional carcinomas lead to neuroendocrine differentiation of cancer cells. Conversely, rare examples of otherwise morphologically typical NET were reported to harbor mutations in two NEC-related genes, *TP53* or *RB1* [10,26,27,29], suggesting that mutations in *TP53* or *RB1* are involved in the progression of well-differentiated NET in some cases [30,31]. Future studies are needed to characterize these outliers with hybrid morphological and genetic features.

In one previous study, MSI was investigated in 89 surgically resected cases of NEC or MiNEN of the esophagus (n = 6), stomach (n = 36), duodenum (n = 4), colorectum (n = 37), gallbladder (n = 3), and pancreas (n = 3) [32]. High MSI was found in 11 cases (12%), including 4 cases of gastric NEC/MiNEN (11% of the gastric cases), a frequency similar to that in the present study. Of note, MSI was a better independent prognostic factor in the entire cohort [32].

A previous deep sequencing study of gastric cancers suggested four distinct molecular groups: Epstein-Barr virus (EBV)-positive (9%), MSI-high (21%), genomically stable (20%), and chromosomal instability types (50%) [21]. EBV-associated gastric carcinoma exhibits unique lymphocyte-rich morphological features, which were not observed in our study cohort. The genomically stable group is characterized morphologically by diffuse infiltrating growth and molecularly by mutations in *CDH1* or *RHOA*. The chromosomal instability type typically has an intestinal-type tubular morphology and *TP53* mutations (>50% of cases) [21]. Mutations in non-*TP53* genes are markedly less common in the last group, similar to our cases. Most cases in our cohort except for the MSI-high MiNEN may correspond to the chromosomal instability type, but this cannot be concluded without chromosomal instability analyses.

In conclusion, the present study revealed that *TP53* is a single, frequently mutated gene in gastric NEC and MiNEN, and alterations in other genes are markedly less common. The molecular features were similar to those of gastric adenocarcinoma. Gene mutations frequently observed in well-differentiated NETs were uncommon but not entirely exclusive.

Author contributions

S.I. contributed to study design, histological analysis, molecular analysis, review of clinical records, and editing the manuscript. M.A., K.F., R.S., H.M., J.S. contributed to Molecular analysis and editing the manuscript. M.K. and T.I. contributed to Histological analysis and editing the manuscript. Y.K. contributed to Clinical workup and editing the manuscript. Y.Z. contributed to study design, histological analysis, interpretation of data, supervising the study, and drafting the manuscript.

References

[1] Chai SM, Brown IS, Kumarasinghe MP. Gastroenteropancreatic neuroendocrine neoplasms: selected pathology review and molecular updates. Histopathology 2018;72:153–67.

[2] Singhi AD, Klimstra DS. Well-differentiated pancreatic neuroendocrine tumours (PanNETs) and poorly differentiated pancreatic neuroendocrine carcinomas (PanNECs): concepts, issues and a practical diagnostic approach to high-grade (G3) cases. Histopathology 2018;72:168–77.

[3] Rindi G, Klimstra DS, Abedi-Ardekani B, Asa SL, Bosman FT, Brambilla E, et al. A common classification framework for neuroendocrine neoplasms: an International Agency for Research on Cancer (IARC) and World Health Organization (WHO) expert consensus proposal. Mod Pathol 2018;31:1770–86.

[4] Yao JC, Hassan M, Phan A, Dagohoy C, Leary C, Mares JE, et al. One hundred years after "carcinoid": epidemiology of and prognostic factors for neuroendocrine tumors in 35,825 cases in the United States. J Clin Oncol 2008;26:3063–72.

[5] Ito T, Igarashi H, Nakamura K, Sasano H, Okusaka T, Takano K, et al. Epidemiological trends of pancreatic and gastrointestinal neuroendocrine tumors in Japan: a nationwide survey analysis. J Gastroenterol 2015;50:58–64.

[6] Pape UF, Berndt U, Muller-Nordhorn J, Bohmig M, Roll S, Koch M, et al. Prognostic factors of long-term outcome in gastroenteropancreatic neuroendocrine tumours. Endocr Relat Canc 2008;15:1083–97.

[7] Rekhtman N, Pietanza MC, Hellmann MD, Naidoo J, Arora A, Won H, et al. Next-generation sequencing of pulmonary large cell

neuroendocrine carcinoma reveals small cell carcinoma-like and non-small cell carcinoma-like subsets. Clin Canc Res 2016;22:3618−29.
[8] George J, Lim JS, Jang SJ, Cun Y, Ozretic L, Kong G, et al. Comprehensive genomic profiles of small cell lung cancer. Nature 2015;524:47−53.
[9] Yachida S, Vakiani E, White CM, Zhong Y, Saunders T, Morgan R, et al. Small cell and large cell neuroendocrine carcinomas of the pancreas are genetically similar and distinct from well-differentiated pancreatic neuroendocrine tumors. Am J Surg Pathol 2012;36:173−84.
[10] Konukiewitz B, Jesinghaus M, Steiger K, Schlitter AM, Kasajima A, Sipos B, et al. Pancreatic neuroendocrine carcinomas reveal a closer relationship to ductal adenocarcinomas than to neuroendocrine tumors G3. Hum Pathol 2018;77:70−9.
[11] Yao J, Garg A, Chen D, Capdevila J, Engstrom P, Pommier R, et al. Genomic profiling of NETs: a comprehensive analysis of the RADIANT trials. Endocr Relat Canc 2019;26:391−403.
[12] Pivovarcikova K, Agaimy A, Martinek P, Alaghehbandan R, Perez-Montiel D, Alvarado-Cabrero I, et al. Primary renal well-differentiated neuroendocrine tumour (carcinoid): next-generation sequencing study of 11 cases. Histopathology 2019;75:104−17.
[13] Ruschoff J, Hanna W, Bilous M, Hofmann M, Osamura RY, Penault-Llorca F, et al. HER2 testing in gastric cancer: a practical approach. Mod Pathol 2012;25:637−50.
[14] Fujikura K, Akita M, Ajiki T, Fukumoto T, Itoh T, Zen Y. Recurrent mutations in APC and CTNNB1 and activated wnt/beta-catenin signaling in intraductal papillary neoplasms of the bile duct: a whole exome sequencing study. Am J Surg Pathol 2018;42:1674−85.
[15] Akita M, Fujikura K, Ajiki T, Fukumoto T, Otani K, Hirose T, et al. Intracholecystic papillary neoplasms are distinct from papillary gallbladder cancers: a clinicopathologic and exome-sequencing study. Am J Surg Pathol 2019;43:783−91.
[16] Akita M, Hong SM, Sung YN, Kim MJ, Ajiki T, Fukumoto T, et al. Biliary intraductal tubule-forming neoplasm: a whole exome sequencing study of MUC5AC-positive and -negative cases. Histopathology 2020.
[17] Jesinghaus M, Konukiewitz B, Keller G, Kloor M, Steiger K, Reiche M, et al. Colorectal mixed adenoneuroendocrine carcinomas and neuroendocrine carcinomas are genetically closely related to colorectal adenocarcinomas. Mod Pathol 2017;30:610−9.
[18] Makuuchi R, Terashima M, Kusuhara M, Nakajima T, Serizawa M, Hatakeyama K, et al. Comprehensive analysis of gene mutation and expression profiles in neuroendocrine carcinomas of the stomach. Biomed Res 2017;38:19−27.
[19] Rossi G, Bertero L, Marchio C, Papotti M. Molecular alterations of neuroendocrine tumours of the lung. Histopathology 2018;72:142−52.
[20] Carethers JM, Jung BH. Genetics and genetic biomarkers in sporadic colorectal cancer. Gastroenterology 2015;149:1177−90. e1173.
[21] The Cancer Genome Atlas Research Network. Comprehensive molecular characterization of gastric adenocarcinoma. Nature 2014;513:202−9.
[22] Cristescu R, Lee J, Nebozhyn M, Kim KM, Ting JC, Wong SS, et al. Molecular analysis of gastric cancer identifies subtypes associated with distinct clinical outcomes. Nat Med 2015;21:449−56.
[23] Jiao Y, Shi C, Edil BH, de Wilde RF, Klimstra DS, Maitra A, et al. DAXX/ATRX, MEN1, and mTOR pathway genes are frequently altered in pancreatic neuroendocrine tumors. Science 2011;331:1199−203.
[24] Wang H, Sun L, Bao H, Wang A, Zhang P, Wu X, et al. Genomic dissection of gastrointestinal and lung neuroendocrine neoplasm. Chin J Canc Res 2019;31:918−29.
[25] Park HY, Kwon MJ, Kang HS, Kim YJ, Kim NY, Kim MJ, et al. Targeted next-generation sequencing of well-differentiated rectal, gastric, and appendiceal neuroendocrine tumors to identify potential targets. Hum Pathol 2019;87:83−94.
[26] Vijayvergia N, Boland PM, Handorf E, Gustafson KS, Gong Y, Cooper HS, et al. Molecular profiling of neuroendocrine malignancies to identify prognostic and therapeutic markers: a Fox Chase Cancer Center Pilot Study. Br J Canc 2016;115:564−70.
[27] Simbolo M, Mafficini A, Sikora KO, Fassan M, Barbi S, Corbo V, et al. Lung neuroendocrine tumours: deep sequencing of the four World Health Organization histotypes reveals chromatin-remodelling genes as major players and a prognostic role for TERT, RB1, MEN1 and KMT2D. J Pathol 2017;241:488−500.
[28] Derks JL, Leblay N, Lantuejoul S, Dingemans AC, Speel EM, Fernandez-Cuesta L. New insights into the molecular characteristics of pulmonary carcinoids and large cell neuroendocrine carcinomas, and the impact on their clinical management. J Thorac Oncol 2018;13:752−66.
[29] Scarpa A, Chang DK, Nones K, Corbo V, Patch AM, Bailey P, et al. Whole-genome landscape of pancreatic neuroendocrine tumours. Nature 2017;543:65−71.
[30] Cros J, Theou-Anton N, Gounant V, Nicolle R, Reyes C, Humez S, et al. Specific genomic alterations in high grade pulmonary neuroendocrine tumours with carcinoid morphology. Neuroendocrinology. 2020.
[31] Tang LH, Untch BR, Reidy DL, O'Reilly E, Dhall D, Jih L, et al. Well-differentiated neuroendocrine tumors with a morphologically apparent high-grade component: a pathway distinct from poorly differentiated neuroendocrine carcinomas. Clin Canc Res 2016;22:1011−7.
[32] Sahnane N, Furlan D, Monti M, Romualdi C, Vanoli A, Vicari E, et al. Microsatellite unstable gastrointestinal neuroendocrine carcinomas: a new clinicopathologic entity. Endocr Relat Canc 2015;22:35−45.